Presynaptic target of Ca^{2+} action on neuropeptide and acetylcholine release in *Aplysia californica*

Kiyoshi Ohnuma, Matthew D. Whim*, Richard D. Fetter†, Leonard K. Kaczmarek‡ and Robert S. Zucker

*Department of Molecular and Cell Biology and †Howard Hughes Medical Institute, University of California, Berkeley, CA 94720, USA, *Department of Pharmacology, University College London, London WC1E 6BT, UK and ‡Department of Pharmacology, Yale University School of Medicine, New Haven, CT 06520, USA*

(Received 19 December 2000; accepted after revision 16 May 2001)

1. When buccal neuron B2 of *Aplysia californica* is co-cultured with sensory neurons (SNs), slow peptidergic synapses are formed. When B2 is co-cultured with neurons B3 or B6, fast cholinergic synapses are formed.
2. Patch pipettes were used to voltage clamp pre- and postsynaptic neurons and to load the caged Ca^{2+} chelator *o*-nitrophenyl EGTA (NPE) and the Ca^{2+} indicator BTC into presynaptic neurons. The relationships between presynaptic $[Ca^{2+}]_i$ and postsynaptic responses were compared between peptidergic and cholinergic synapses formed by cell B2.
3. Using variable intensity flashes, Ca^{2+} stoichiometries of peptide and acetylcholine (ACh) release were approximately 2 and 3, respectively. The difference did not reach statistical significance.
4. ACh quanta summate linearly postsynaptically. We also found a linear dose–response curve for peptide action, indicating a linear relationship between submaximal peptide concentration and response of the SN.
5. The minimum intracellular calcium concentrations ($[Ca^{2+}]_i$) for triggering peptidergic and cholinergic transmission were estimated to be about 5 and 10 μM, respectively.
6. By comparing normal postsynaptic responses to those evoked by photolysis of NPE, we estimate $[Ca^{2+}]_i$ at the release trigger site elicited by a single action potential (AP) to be at least 10 μM for peptidergic synapses and probably higher for cholinergic synapses.
7. Cholinergic release is brief (half-width ~200 ms), even in response to a prolonged rise in $[Ca^{2+}]_i$, while some peptidergic release appears to persist for as long as $[Ca^{2+}]_i$ remains elevated (for up to 10 s). This may reflect differences in sizes of reserve pools, or in replenishment rates of immediately releasable pools of vesicles.
8. Electron microscopy revealed that most synaptic contacts had at least one morphologically docked dense core vesicle that presumably contained peptide; these were often located within conventional active zones.
9. Both cholinergic and peptidergic vesicles are docked within active zones, but cholinergic vesicles may be located closer to Ca^{2+} channels than are peptidergic vesicles.

Many neurons contain both classical transmitters, such as ACh and glutamate, as well as peptide co-transmitters (Kupfermann, 1991). There are some differences in the secretion of these two types of transmitters. For instance, release of classical transmitters can occur with a single AP, whereas peptide secretion often requires high frequency bursts of activity (Dutton & Dyball, 1979; Jan & Jan, 1982; Whim & Lloyd, 1989; Cropper *et al.* 1990; Peng & Horn, 1991; but see Whim *et al.* 1997). Thus, the relationship between transmitter release and $[Ca^{2+}]_i$ may differ between the two transmitter types. With classical transmitters, the amount of transmitter release depends on the third to fourth power of extra- or intracellular $[Ca^{2+}]$ (Dodge & Rahamimoff, 1967; Katz & Miledi, 1970; Dudel, 1981; Augustine *et al.* 1985; Heidelberger *et al.* 1994; Landò & Zucker, 1994). This highly non-linear relationship was attributed to three or four successive Ca^{2+} ions binding to an as yet unspecified target to trigger transmitter release. In contrast, synaptic peptide release appears to depend linearly on $[Ca^{2+}]_i$ (Sakaguchi *et al.*

1991; Peng & Zucker, 1993). The calcium stoichiometry of release from non-neural peptidergic cells has been reported to be higher (Thomas *et al.* 1993; Proks *et al.* 1996). In addition, although the $[Ca^{2+}]_i$ needed to release classical transmitters is estimated to approach or even exceed 100 μM (Roberts *et al.* 1990; Adler *et al.* 1991; Llinás *et al.* 1992; Landò & Zucker, 1994), the $[Ca^{2+}]_i$ required to release peptide transmitters has been suggested to be about 1 μM (Cazalis *et al.* 1987; Lindau *et al.* 1992; Peng & Zucker, 1993). Small clear vesicles containing classical transmitters cluster and attach to the presynaptic membrane and form active zones. However, peptide secretion is believed not to occur at active zones (De Camilli & Jahn, 1990; Golding, 1994; Leenders *et al.* 1999).

Comparing peptidergic and classical synapses is difficult, because differences may arise from the different cells releasing the two transmitter types, or from essential differences in the transmitter releasing systems. Whim *et al.* (1997) produced both peptidergic and cholinergic synapses using the same buccal ganglion neuron, B2, from *Aplysia*. This neuron synthesizes and releases ACh (Lloyd *et al.* 1985) and the small cardioactive peptides A and B (SCP_A and SCP_B; SCPs) (Lloyd *et al.* 1986), which are localized to dense-core vesicles (DCVs) (Kreiner *et al.* 1986; Reed *et al.* 1988). When B2 (or B1) is co-cultured with a SN, a slow peptidergic synapse forms. However, when B2 is co-cultured with neuron B3 (or B6), a cholinergic synapse forms (Whim *et al.* 1997). Although this peptidergic synapse behaves similarly to other peptidergic synapses, it has a unique property: a single AP is sufficient to induce a postsynaptic response when making a soma–soma synapse (Whim *et al.* 1997).

Using photolabile Ca^{2+} chelators to manipulate $[Ca^{2+}]_i$, we have compared the Ca^{2+} sensitivities of the presynaptic targets mediating peptide and classical transmitter release as detected by the choice of postsynaptic partner. Although clear differences were seen between them, the differences were smaller than expected. Electron microscopy of peptidergic synapses revealed that they also have classical synapses containing active zone structures. The identification of peptidergic active zones is novel, and may explain the ability of a single AP to evoke a postsynaptic response.

METHODS

Cell culture

Cells were isolated and maintained by standard techniques (Schacher & Proshansky, 1983; Whim *et al.* 1997). *Aplysia californica* weighing ~1 g and ~100 g were anaesthetized by injection of isotonic $MgCl_2$ and used for buccal and pedal-pleural ganglia, respectively. Ganglia were removed and incubated in 1% protease (Sigma type IX) in sterile normal artificial seawater (NASW) at 34°C for 1.5 or 2.5 h, respectively. Neurons were removed using finely pulled glass probes and maintained in sterile culture medium at room temperature (20–22°C). The medium consisted of 26% *Aplysia* haemolymph; 4% fetal bovine serum; 70% NASW, supplemented with penicillin (50 u ml^{-1}), streptomycin (50 μg ml^{-1}), vitamin mixture (0.5× minimal essential medium (MEM)), and non-essential (0.2× MEM) and essential amino acids without L-glutamine (0.2× MEM). Although fetal bovine serum was added to suppress electrical coupling (Carrow & Levitan, 1989), strong electro-coupling sometimes occurred. Such cell pairs were not used for experiments. Neurons generally could be identified by visual criteria alone (Church *et al.* 1993; Whim & Lloyd, 1994), and any anomalous ganglia were rejected. The NASW contained (mM): 460 NaCl, 10.4 KCl, 55 $MgCl_2$, 11 $CaCl_2$ and 15 Na-Hepes (pH 7.5: ~1070 mosmol kg^{-1}).

All of the experiments used the cultured soma–soma synapse configuration (Haydon, 1988; Whim *et al.* 1997). Buccal B2, B3, and B6 neurons, and the pleural SNs were isolated and separately maintained in droplets of culture medium on dishes. After more than 1 day the primary neurite had been reabsorbed, and the pre- and postsynaptic cells were joined. The neurons adhered to each other and were used 1–4 days later. Cholinergic pairs consisted of presynaptic B2 and postsynaptic B3 or B6 (to simplify, we call this B2–B3) and peptidergic pairs consisted of presynaptic B2 and postsynaptic SN (B2–SN). Although there was no difference between B3 and B6 as ACh detectors (Whim *et al.* 1997; Kehoe & McIntosh, 1998), B3 neurons were mainly used. B3 are bigger than B2 neurons and can be more easily distinguished from B2 after combination. For recording, neuron pairs were transferred to a glass-bottomed experimental chamber. Although we did not observe any differences in the calcium dependency of transmission between B2–B3 and B2–B6 or between B1–SN and B2–SN, we cannot rule out the possibility that the postsynaptic target cell could modify the characteristics of transmitter release.

Electrical recordings

Whole-cell voltage-clamp recordings of both the presynaptic and the postsynaptic neurons were performed with an EPC-9 double patch-clamp amplifier (EPC-9/2) with PULSE software (HEKA, Lambrecht/Pfalz, Germany).

Two types of patch pipettes and filling solutions were used. One type of pipette (outer diameter of the tip ~2 μm) had resistances of ~1 MΩ measured in NASW, and was used with the normal pipette solution containing (mM): 435 potassium asparate, 70 KCl, 11 glucose, 10 potassium glutathione, 5 Na_2-ATP, 0.1 GTP, 1.2 $MgCl_2$, 5 K-Hepes (pH 7.3: ~1050 mosmol kg^{-1}). Gigohm seals were obtained using this pipette and solution. A second type of pipette had a resistance of ~0.3 MΩ (outer diameter of the tip ~5 μm), and was used for loading BTC and NPE into the presynaptic neuron. The filling solution contained (mM): 416 potassium asparate, 70 KCl, 11 glucose, 10 potassium glutathione, 5 Na_2-ATP, 0.1 GTP, 1.2 $MgCl_2$, 0.25 BTC, 5 NPE, 3.75 $CaCl_2$ (75% of NPE), 50 K-Hepes (pH 7.3; ~1050 mosmol kg^{-1}). Using this pipette, we obtained seal resistances up to 200 MΩ. The holding potential of presynaptic B2 was −46 mV. The holding potential of postsynaptic SN was −31 mV and that of postsynaptic B3 was −36 mV because it was sometimes unstable at −31 mV.

The liquid junction potential of the extracellular solution against the internal solution was measured to be +7 mV, and all clamp potentials were corrected accordingly. Experiments were performed at room temperature.

$[Ca^{2+}]_i$ measurement and elevation

After mounting the experimental chamber onto the stage of an upright IX 70 microscope (Olympus, Tokyo, Japan), the chamber was perfused with NASW. $[Ca^{2+}]_i$ was measured by the dual-wavelength ratiometric method using BTC (Iatridou *et al.* 1994), which was excited with light alternated between 400 and 480 nm using a Polychrome II monochrometer (TILL Photonics, Martinsried, Germany), and the resulting fluorescence signal at wavelengths greater than 510 nm was measured using an R928 photo-multiplier

Table 1. Solutions used to calibrate BTC with NPE under high ionic strength

	Concentrations (mM)				
	A	B	C	D	E
K-Asparate* [1.23]	300	300	305	310	360
KCl	65	65	65	65	10
K-Hepes (pH 7.3)	150	150	150	150	150
Glucose	11	11	11	11	11
K_2-Glutathione	10	10	10	10	10
$CaCl_2$	0	7.5	25	35	45
K_3-DPTA* [4.5]	0	50	50	50	0
K_2-EGTA* [~7]	50	0	0	0	0
BTC*	0.25	0.25	0.25	0.25	0.25
NPE* [~7] ($CaCl_2$)	5 (0)	5(5)	5(5)	5(5)	5(5)
	Measured $[Ca^{2+}]$ (μM)				
	A	B	C	D	E
111 % solution	< 0.01	5.88	33.1	74.6	6440
Pre-flash	< 0.01	5.95	33.1	74.5	6320
Post-flash	< 0.01	7.52	37.9	87.4	6610

Top part of table shows composition of calibration solutions A–E. * Ca^{2+}-binding compound with pK values shown in square brackets. Bottom part of table shows measured $[Ca^{2+}]$ in the 111 % solution containing the first eight constituents and used to make final solutions, or calculated using pK values in final solutions before (Pre-flash) and after (Post-flash) single full strength (no neutral density filter) photolysis of NPE.

tube (PMT; Hamamatsu, Shizuoka, Japan). We used a UApo/340 objective (×40, n.a. = 1.35, oil immersion, Olympus), a 505 DC XR-UV dichroic mirror, and HQ 535/50 emission filter (Chroma Technology Co., Brattleboro, VT, USA). The excitation light exposed a 50 μm square region, which included the entire presynaptic neuron. The fluorescence intensity was measured from a 40 μm square region centred within the excitation region.

$[Ca^{2+}]_i$ was determined from the ratio (R) of the fluorescence signals at both wavelengths, according to (Grynkiewicz *et al.* 1985):

$$[Ca^{2+}]_i = K_{dApp}[(R - R_{min})/(R_{max} - R)], \quad (1)$$

where K_{dApp} is the apparent dissociation constant, R_{min} is the minimum ratio in zero Ca^{2+}, and R_{max} is the maximum ratio at saturated Ca^{2+}. These calibration constants were obtained from in-cuvette calibrations.

To obtain instantaneous increases in $[Ca^{2+}]_i$, 75 % Ca^{2+}-loaded NPE (Ellis-Davies & Kaplan, 1994) was perfused into the presynaptic neuron from the patch pipette, and 200 J discharge flashes of UV light were applied to the whole presynaptic area (100 μm square) by fibre-optic coupling through a dual port condenser that used a sapphire mirror to combine photolysis light at 92 % transmittance and fluorescence excitation light at 8 % reflectance. The flash-lamp was a modified Chadwick-Helmuth system (El Monte, CA, USA) described previously (Landò & Zucker, 1989; Zucker, 1994). A single 200 J discharge of UV flash with 0.3 neutral density filter photolysed 50 % of DM-nitrophen half-loaded with Ca^{2+}, measured in micro-cuvettes on the microscope stage as described previously (Zucker, 1993). Flash intensity was sometimes reduced with neutral-density (ND) filters transmitting between 12 and 76 %.

Calibrations of BTC with NPE

In-cuvette calibrations under high ionic strength (500–600 mM) were performed in the presence of NPE, using the Ca^{2+} buffer 1,3-diaminopropan-2-ol-tetraacetic acid (DPTA) to control moderate $[Ca^{2+}]$ (Neher & Zucker, 1993). First, because aspartate binds Ca^{2+}, the pK of aspartate was measured. $[Ca^{2+}]$ in a solution containing 350 mM aspartate and 175 mM $CaCl_2$ (pH = 7.3) was measured at 59 mM with a Ca^{2+}-sensing electrode (MI-600, Microelectrodes, Inc., Bedford, NH, USA). Second, 111 % concentrated solutions containing the top eight chemicals listed in Table 1 (excluding BTC and NPE) were made. Using a Ca^{2+}-sensing electrode, $[Ca^{2+}]$ of those solutions was measured and from this and the known buffering effect of aspartate, the dissociation constant (pK) of DPTA was calculated (Table 1). Third, 10 times concentrated solutions containing BTC and NPE were made and mixed in a ratio of 1:9 with the 111 % concentrated solutions to make small volumes of final calibration solutions A–E (Table 1). In all but the zero-Ca^{2+} solution, NPE was complexed with Ca^{2+} to prevent distortion of the $[Ca^{2+}]$ level set by DPTA. $[Ca^{2+}]$ of those solutions were calculated using our measured pK values of aspartate and DPTA, and published values for NPE (Ellis-Davies & Kaplan, 1994). Finally, rectangular glass cuvettes (50 μm path length, VitroCom, Mountain Lakes, NJ, USA) filled with the calibration solutions A–E were put in glass-bottomed chambers and covered with light mineral oil. Fluorescence ratios were measured on the microscope and fitted to eqn (1) to calculate calibration constants.

The results are shown in Fig. 1. Before UV photolysis, the dissociation constant (K_d) was 19.4 μM, K_{dApp} was 158 μM, and R_{max}/R_{min} was 24.7. After a single 100 % flash photolysis (no ND filter), K_d was 20.1 μM, K_{dApp} was 146 μM, and R_{max}/R_{min} was 22.6. Our measurement of K_d is within the range of published values (Iatridou *et al.* 1994; Zhao *et al.* 1996). Although there was a small caged chelator–indicator interaction (Zucker, 1992; Neher & Zucker, 1993; Kasai *et al.* 1996), the effect was negligible, especially under 40 μM. We used the post-flash value to calculate $[Ca^{2+}]_i$.

We also performed *in situ* calibrations. Calibration solutions were like the solutions listed in Table 1 but with Cs^+ substituted for K^+. Calibration solutions were loaded into the SN using a patch pipette. *In situ* calibration results are close to in-cuvette results at some points (Fig. 1), but these were not used to calculate calibration constants.

There were several problems. Because the neuron has high volume (about 50 μm in diameter and spherical), gradual filling from the patch pipette causes the fluorescence ratio to reach a plateau very slowly (more than 30 min). The ratio was often lower than expected, because $[Ca^{2+}]_i$ never reached the level of the pipette solution due to cellular Ca^{2+} uptake and extrusion processes. We tried using lithium-substituted ASW to suppress the Na^+–Ca^{2+} exchanger, but it had little effect. Furthermore, especially when high $[Ca^{2+}]_i$ solutions were introduced, most neurons lost membrane integrity as indicated by a sudden increase in fluorescence ratio before that ratio and $[Ca^{2+}]_i$ approached steady levels during perfusion from the patch pipette. In such cases, the sudden ratio increase probably reflected membrane breakdown and Ca^{2+} inflow. Due to this problem it was impossible to obtain any data at all at the highest $[Ca^{2+}]_i$ levels, and the *in situ* data we did obtain did not show a clear sign of saturation as $[Ca^{2+}]_i$ increases, preventing estimation of K_{dApp} or R_{max} from this data. The fact that fluorescence ratios were still rising when cells were lost indicates that fluorescence ratios for *in situ* calibrations underestimate the true values, especially at higher $[Ca^{2+}]_i$ levels. This is exactly what a comparison of the *in situ* and cuvette data shows, and so we think the *in situ* results are consistent with (and essentially validate) the more accurate cuvette measurements.

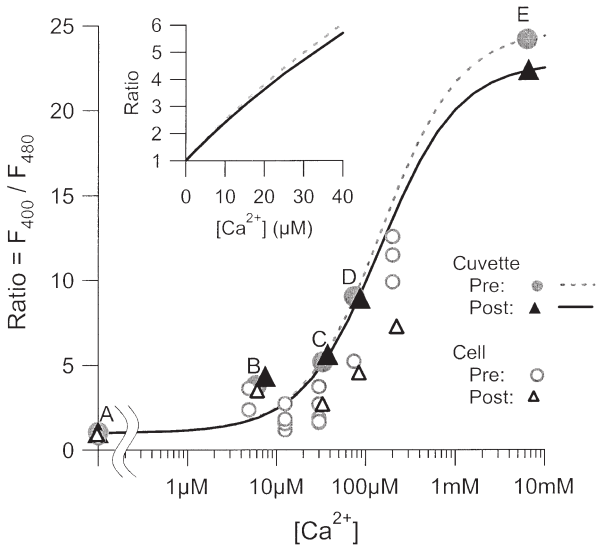

Figure 1. BTC calibration curves with NPE under high ionic strength (about 550 mM) before and after UV flash photolysis

Fluorescence ratios were normalized by R_{min} before photolysis and plotted on a semi-log scale. The filled circles represent in-cuvette pre-photolysis measurements and the filled triangles represent post-photolysis fluorescence ratios (no ND filter; see text). The letters (A–E) represent solution names (see Table 1); the leftmost point is in nominally zero-Ca^{2+} medium. Lines are best-fit curves to in-cuvette values based on eqn (1) (dashed line: pre-flash, continuous line: post-flash). Inset shows a high magnification view at low concentration with linear scales. Most of the experiments were done in this range. Because the point around 10 μM (solution B) fell above the curve, we did not include it in calculating calibration values. Although these two curves are slightly different because of caged chelator–indicator interactions (Zucker, 1992), the difference is negligible at low Ca^{2+} concentrations. We used the post-flash value ($K_d = 20$ μM) to convert fluorescence ratios to $[Ca^{2+}]_i$ resulting from NPE photolysis. *In situ* ratios are represented as the open circles (pre-flash) and as the open triangles (post-flash).

When in-cuvette calibration R_{min} was used, the resting (pre-flash) $[Ca^{2+}]_i$ of presynaptic neurons was occasionally estimated at a negative value, and at other times as high as 2 μM. These cells were perfused with a Ca^{2+}-loaded Ca^{2+} buffer (NPE) which should have buffered $[Ca^{2+}]_i$ to 0.4 μM, which is the level of $[Ca^{2+}]_i$ that we both calculated and measured in the presynaptic filling solution (using Ca^{2+}-sensitive electrodes). At low values of R, negative estimates of $[Ca^{2+}]_i$ can only arise from errors in R_{min}, and the largest deviations we observe from 0.4 μM would arise from errors of about 20–25 % in R_{min}. Variation in R_{min} probably arises from variability in the colour of excitation light, in which case R_{max} should covary with R_{min}. Therefore, R_{min} was adjusted to set the resting $[Ca^{2+}]_i$ equal to 0.4 μM, and R_{max} was adjusted to keep the ratio R_{max}/R_{min} constant. This procedure is similar to that used in earlier studies employing low-affinity dyes (e.g. Heinemann *et al.* 1994).

We also tried using dimethoxynitrophenyl-EGTA-4 (DMNPE-4) to try to produce higher $[Ca^{2+}]$ rises than are possible with NPE. The efficiency of uncaging DMNPE-4 should be five times higher than for NPE (Ellis-Davies & Kaplan, 1994; DelPrincipe *et al.* 1999). In addition, because it has higher affinity for Ca^{2+} than NPE before photolysis, this chelator can be loaded with more Ca^{2+} than NPE at resting free $[Ca^{2+}]_i$ levels. We performed in-cuvette calibrations of BTC with DMNPE-4. The pre-flash calibration constants were almost the same as those with BTC alone. However, the post-flash values changed dramatically: K_d decreased to 65 %, K_{dApp} decreased to 60 %, R_{min} decreased to 87 %, and R_{max} decreased to 59 %. Even with corrected values for calibration constants, the $[Ca^{2+}]_i$ did not rise as much as expected on photolysis of DMNPE-4. Thus, the light sensitivity of DMNPE-4 was less than expected, and there was a large DMNPE-4–indicator interaction, which made it very difficult to estimate $[Ca^{2+}]$ changes accurately after photolysis (Zucker, 1992; Neher & Zucker, 1993). It is possible that these problems are particular to the samples of DMNPE-4 and BTC available to us, but because of them we decided not to pursue the use of DMNPE-4 in our preparation.

Puffing SCP_B onto SNs

Using a U-shaped tube with gravity feed and electrical valve control (Krishtal & Pidoplichko, 1980; Fenwick *et al.* 1982), SCP_B was puffed onto a SN. The speed of concentration change was measured by puffing diluted (85 %) NASW onto the SN and measuring changes in liquid junction potential in an adjacent electrode. The 10–90 % rise time of solution change was 0.18 ± 0.03 s (mean ± S.E.M.), which is faster than the initiation of a peptidergic response in SN (Fig. 5).

Electron microscopy

B2–SN cell pairs were cultured on Aclar film (Ted Pella Inc., Redding, CA, USA), a tissue culture substrate that can be sectioned for electron microscopy. The cell pairs remained tightly adhered to the Aclar film during fixation, processing and embedding, thus maintaining the orientation of the cells and allowing their identification in tissue blocks and thin sections.

Cell pairs were fixed with 2 % glutaraldehyde or 2 % glutaraldehyde–1 % formaldehyde in 0.1 M sodium cacodylate buffer, pH 7.4 for 2 h at room temperature. Following this primary fixation, the specimens were post-fixed with 1 % OsO_4 in 0.1 M sodium cacodylate buffer, stained *en bloc* with 1 % uranyl acetate in distilled water, dehydrated in a graded ethanol series and embedded in Eponate 12 (Ted Pella, Inc.).

Serial 80–85 nm sections were cut with a Reichert-Jung Ultracut E ultramicrotome (Leica, Deerfield, IL, USA) and mounted on formvar-coated slot grids. The plane of sectioning was oriented perpendicular to the plane of contact between the cell pairs, and block faces were trimmed asymmetrically so the SN and B2 cells could be easily and uniquely identified in the electron microscope. Following sequential staining with uranyl acetate and Sato's lead (Sato, 1968), the sections were examined and photographed on a 1200EX/II electron microscope (JEOL, Tokyo, Japan) operating at 80 kV.

The distribution of vesicles as a function of distance from active zone membranes in the presynaptic bouton-like contacts was examined in 34 serial section micrographs of four B2–SN cell pairs. We measured the minimal distance between all synaptic vesicles and the electron dense membrane specialization of the active zone out to a distance of 1000 nm from the active zone membrane (Hess *et al.* 1993; Reist *et al.* 1998). The presynaptic bouton-like contacts used in these vesicle counts were slightly oblong in shape, measuring 2.3–4.4 μm in length and 2.0–3.3 μm in width.

Drugs

The caged Ca^{2+} chelators NPE and DMNPE-4 were gifts from Dr G. C. R. Ellis-Davies (Medical College of Pennsylvania Hahnemann University). BTC was obtained from Molecular Probes, Inc. (Eugene, OR, USA). α-Conotoxin IMI was obtained from BACHEM (Torrance, CA). SCP_B was obtained from American Peptide Company (Sunnyvale, CA, USA). DPTA, protease type IX (bacterial), tetrodotoxin, and penicillin–streptomycin (lyophilized) were obtained from Sigma (St. Louis, MO, USA). MEM amino acids solution without L-glutamine solution (50 ×), MEM non-essential amino acid solution (100 ×), MEM vitamin mixture (lyophilized), and fetal bovine serum were obtained from GIBCO BRL (Grand Island, NY, USA).

Presentation of data

Results are expressed as means ± S.E.M.

RESULTS

Cholinergic and peptidergic release evoked by a depolarising pulse

Figure 2 shows examples of cholinergic (B2–B3) and peptidergic (B2–SN) postsynaptic currents (PSCs) evoked by a single 5 ms depolarisation to 19 mV. The postsynaptic responses show a sharp threshold to gradual increases in pulse potential, are unaffected by prolongation of the pulse, and are blocked by 100 μM tetrodotoxin, and are therefore mediated by APs in unclamped presynaptic processes. Depolarizations of 5 ms evoke single APs in *Aplysia* neurons, where typical AP duration is ~5–10 ms and refractory period is ~20 ms (unpublished observations).

Transmission at these synapses has been studied by Whim *et al.* (1997). Cholinergic transmission is inhibitory and involves opening of Cl^- channels (Gardner & Kandel, 1977), while peptidergic transmission is excitatory and involves second messenger-mediated closing of K^+ channels, which are normally open (Ocorr & Byrne, 1985; Baxter & Byrne, 1989). Using postsynaptic perfusion of a solution with 72 mM Cl^- and 550 mM K^+, and NASW as a bathing solution with 600 mM Cl^- and 10 mM K^+, the cholinergic and peptidergic transmission have reversal potentials of −53 and −100 mV, respectively. Recording postsynaptic responses under voltage clamp around −35 mV, cholinergic opening of Cl^- channels produces a Cl^- influx or outward current while peptidergic closing of K^+ channels reduces K^+ efflux and produces an inward current (Ocorr & Byrne, 1985). The responses are also

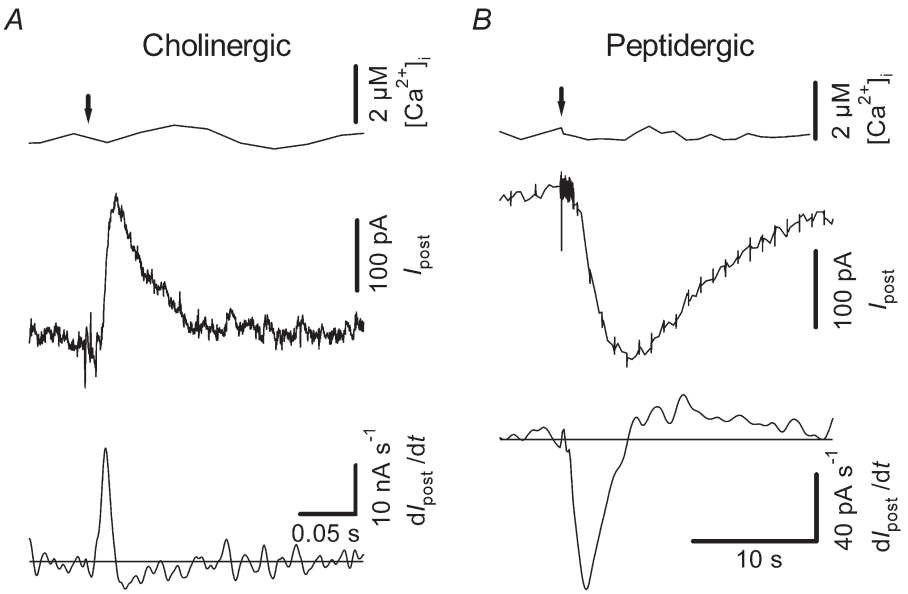

Figure 2. Cholinergic and peptidergic PSCs evoked by an AP

Upper trace, presynaptic $[Ca^{2+}]_i$; middle trace, postsynaptic current (I_{post}); lower trace, rate of I_{post} change evoked by a single presynaptic 5 ms depolarisation (arrow) from −46 mV to +19 mV in cholinergic (*A*, B2–B3) and peptidergic (*B*, B2–SN) cell pair. The volume averaged presynaptic (soma) $[Ca^{2+}]_i$ change was undetectable during a 5 ms depolarising pulse evoking a single AP. This suggests that both cholinergic and peptidergic release are evoked by local regions of submembrane $[Ca^{2+}]_i$.

Table 2. Differences in Ca^{2+} action on cholinergic and peptidergic secretion

	Cholinergic	Peptidergic
Ca^{2+} stoichiometry	3.1 ± 0.5 (6)	2.2 ± 0.6 (8)
Maximum rate of PSC change (nA s^{-1})		
$[Ca^{2+}]_i = 10\ \mu M$	3.6 ± 1.9 (6)	0.047 ± 0.015 (8)
Action potential	48 ± 21 (8)	0.035 ± 0.014 (10)
Minimum $[Ca^{2+}]_i$ (μM) eliciting release with transmission probability > 0.5	10	5
$[Ca^{2+}]_i$ (μM) elicited by an action potential at release site	23	8.8

Number of measurements is shown in parentheses. Upper two rows came from flash photolysis experiments. The bottom row was calculated based on upper three rows using eqn (4).

distinguishable kinetically. Cholinergic inhibitory postsynaptic currents (IPSCs) start after a synaptic delay of a few milliseconds following presynaptic depolarisation and last only about 0.1 s. This is at least five times faster than the desensitisation rate of the desensitising component of cholinergic responses (Kehoe & McIntosh, 1998), and so apparently reflects the duration of the release of transmitter. Excitatory synaptic currents (EPSCs), which are at least partially, and perhaps wholly, due to release of SCPs (Whim *et al.* 1997), start about 1 s after presynaptic depolarisation and last for more than 10 s. The slow decay of peptidergic responses reflects, at least in part, the slow kinetics of postsynaptic processes (Ocorr & Byrne, 1985; Baxter & Byrne, 1989); indeed, postsynaptic responses to brief application of peptide decay at a similar rate (Fig. 5*B*). The maximum rates of PSC change (peak dI_{post}/dt) of both synaptic types are shown in Table 2.

The presynaptic filling solution contained BTC and NPE, allowing us to measure $[Ca^{2+}]_i$ and elevate $[Ca^{2+}]_i$ by flash photolysis of NPE. We were unable to detect a presynaptic $[Ca^{2+}]_i$ increase elicited by a single AP (Fig. 2). Because PSCs are abolished in a low-Ca^{2+}, high-Mg^{2+} ASW

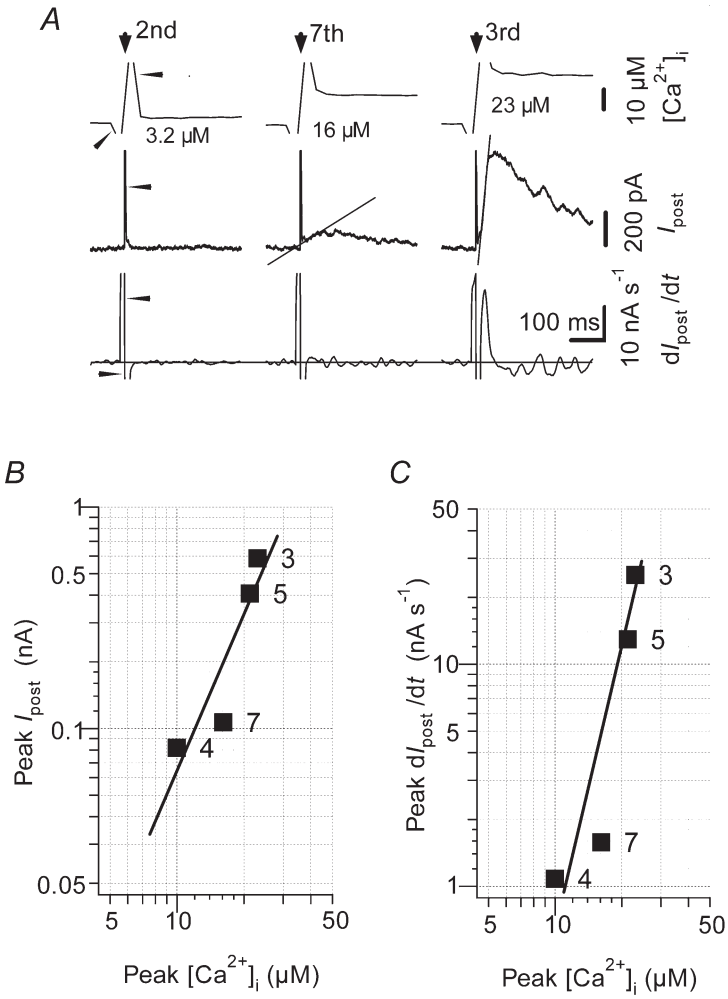

Figure 3. Stoichiometry of Ca^{2+} action in cholinergic synapse (B2–B3)

A, presynaptic $[Ca^{2+}]_i$ (upper traces), cholinergic IPSCs (middle traces), and their derivatives (lower traces) evoked by flash photolysis (arrow) of different intensities in a single cell pair. The numbers represent sequence of flashes. Straight lines in middle traces are best-fit lines providing an alternative estimate of maximum rate of current change (peak dI_{post}/dt). Under- and overshoot (arrowheads in left trace) are flash artefacts. Peak I_{post} (in *B*) and peak dI_{post}/dt (in *C*) from the same cell pair as in *A* were plotted against peak $[Ca^{2+}]_i$ on log–log scales. The number beside each point represents sequence of flashes. The straight line is the best fit to these data using eqn (3). There is no order dependence so the results are not distorted by history-dependent enhancement or depression of release. Stoichiometry of Ca^{2+} action was determined from the average slope of best fitting lines of 6 such experiments as 2.6 ± 0.3 in *B* and 3.1 ± 0.5 in *C*.

(Whim *et al.* 1997), transmitter release is dependent upon Ca^{2+} entry, and depolarisation in NASW should cause presynaptic $[Ca^{2+}]_i$ to rise. However, since fluorescence was measured from the whole presynaptic neuronal area (40 μm square) using a conventional microscope and PMT, only the volume-averaged $[Ca^{2+}]_i$ change could be assessed, i.e. local $[Ca^{2+}]_i$ changes at putative transmitter release sites were not detectable. The results suggest that both cholinergic and peptidergic release are evoked by local regions of presynaptic submembrane $[Ca^{2+}]_i$ increases.

Stoichiometry of Ca^{2+} action at cholinergic synapses (B2–B3)

IPSCs evoked by flash photolysis of presynaptic NPE were measured. After establishing whole-cell voltage clamp of both pre- and postsynaptic neurons, we waited 15–30 min for BTC and NPE to diffuse into B2, and then applied flashes of different intensities using ND filters to elevate $[Ca^{2+}]_i$ uniformly throughout the presynaptic neuron. Between flashes, we waited at least 150 s for recovery of the presynaptic $[Ca^{2+}]_i$ and the postsynaptic current to pre-flash levels.

Figure 3*A* shows three examples of flash-evoked presynaptic $[Ca^{2+}]_i$ rise and IPSCs. A dim flash had little effect on presynaptic $[Ca^{2+}]_i$, and no IPSCs were seen. Higher $[Ca^{2+}]_i$ rises evoked by brighter flashes elicited clear IPSCs. The postsynaptic response was very brief (time to peak for the brightest flashes about 50 ms, decay half-time about 150 ms) compared to the duration of $[Ca^{2+}]_i$ elevation (half-width about 10 s, see Fig. 4*A*). Thus the rapid phase of transmitter release was over within 50 ms, suggesting the rapid release of a pool of docked vesicles. Flash-evoked IPSCs were somewhat broader than those evoked by APs (Fig. 2*A*: time to peak about 25 ms, decay half-time about 25 ms), probably because the uniform elevation of $[Ca^{2+}]_i$ in photolysis experiments avoids the rapid diffusion of Ca^{2+} ions from Ca^{2+} channels in active zones occurring during APs. Thus, in AP-evoked release, the duration of the $[Ca^{2+}]_i$ transient in active zones may be partially rate limiting, and the IPSC is more like the response to a brief pulse of $[Ca^{2+}]_i$, while in flash photolysis experiments, the IPSC is a response to a step rise in $[Ca^{2+}]_i$, consisting of an initial exocytic burst followed by a low rate of release lasting for several hundred milliseconds.

We considered two ways to estimate the stoichiometry of Ca^{2+} action in releasing transmitter. In the first, we plotted peak response amplitude (postsynaptic current,

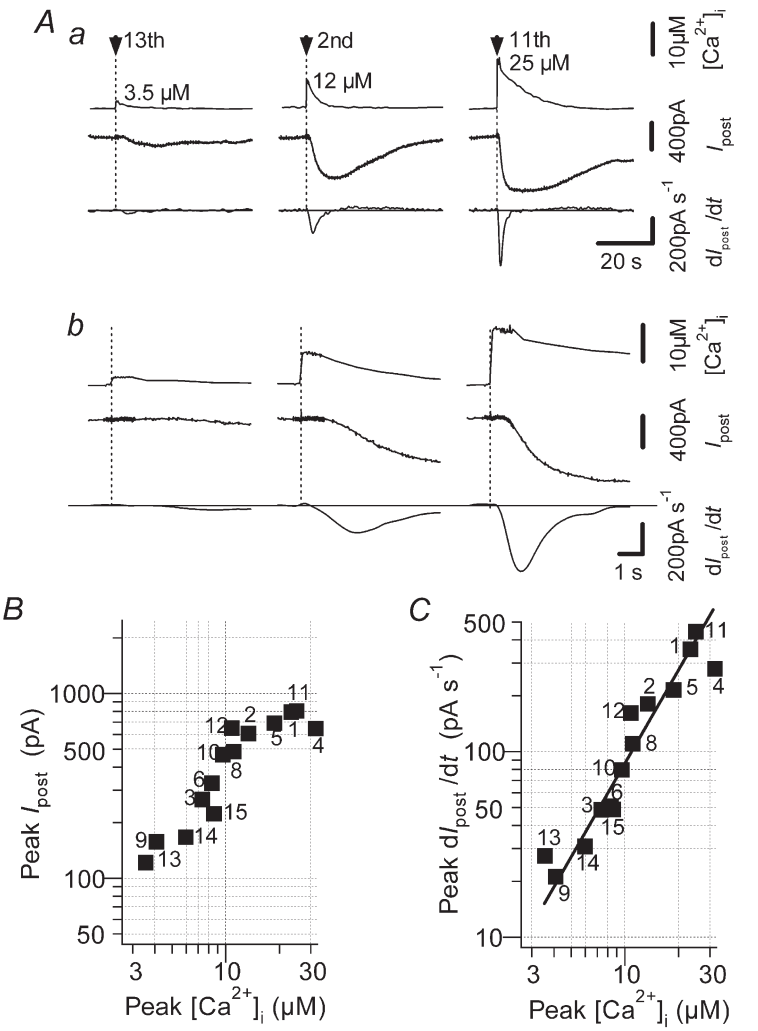

Figure 4. Stoichiometry of Ca^{2+} action in peptidergic synapse (B2–SN)

Aa, presynaptic $[Ca^{2+}]_i$ (upper traces), peptidergic EPSCs (I_{post}: middle traces), and rate of I_{post} change (lower traces) evoked by different intensities of flash photolysis (arrow; the numbers represent sequence of flashes). *Ab*, the same responses on a faster time scale. Peak I_{post} (in *B*) and absolute value of peak dI_{post}/dt (in *C*) from the same cell pair as in *A* were plotted against peak $[Ca^{2+}]_i$. The number beside each point represents sequence of flashes, and no order dependence or sign of synaptic enhancement or depression was observed. Because I_{post} was saturated above 10 μM, stoichiometry of Ca^{2+} action was determined only from the maximum dI_{post}/dt, estimated from the slope of the best-fitting line using eqn (3) (as shown by the line in C). The average stoichiometry from 8 such experiments was 2.2 ± 0.6 ($n = 8$).

I_{post}) *vs.* peak presynaptic $[Ca^{2+}]_i$ using log–log coordinates (Fig. 3*B*). Exhaustion of a finite pool size before the peak of a response might cause the maximum amplitude of flash-evoked responses to saturate at large $[Ca^{2+}]_i$. For this reason, we also plotted the maximum rate of change of postsynaptic current (peak dI_{post}/dt) *vs.* $[Ca^{2+}]_i$ (Fig. 3*C*). Peak dI_{post}/dt occurs early in the response (within the first 20 ms, see Fig. 3*A*), should not be affected by pool exhaustion or adaptation-like processes (Hsu *et al.* 1996) occurring later in the response, and in any case should be a better measure of maximum rate of transmitter release. Although peak dI_{post}/dt ought to be proportional to maximum rate of transmitter release, neither $I_{post}(t)$ nor $dI_{post}(t)/dt$ provide an accurate measure of the full time course of transmitter release, because of distortions imposed by postsynaptic receptor kinetics and diffusion of transmitter. We were unable to detect miniature IPSCs (probably due to the low input resistance of the large postsynaptic cells), and so could not use a convolution method to estimate time course of release (Van der Kloot, 1988). Thus it is not possible to obtain time constants of the decay of secretion from our data, except to estimate them to have an order of magnitude in the low tens of milliseconds or faster.

Using either measure, the relationship between $[Ca^{2+}]_i$ and maximum release rate was highly non-linear. Stoichiometry (N) was assessed by fitting our estimate of maximum release rate *vs.* $[Ca^{2+}]_i$ to the reaction equation (Dodge & Rahamimoff, 1967; Dudel, 1981):

$$\text{Release rate} \propto \{[Ca^{2+}]_i/(1 + [Ca^{2+}]_i/K)\}^N, \quad (2)$$

where K reflects saturation of not only the presynaptic Ca^{2+} binding site and all subsequent reactions involved in triggering transmitter release, but also all processes involved in generating postsynaptic responses. At low $[Ca^{2+}]$ levels, below saturation of postsynaptic responses ($[Ca^{2+}]_i \ll K$), eqn (2) can be simplified to

$$\log(\text{release rate}) \propto N \log[Ca^{2+}]_i. \quad (3)$$

N was determined by the slope of the log–log plot (Fig. 3*B*). By estimating the release rate from peak I_{post}, N was 2.6 ± 0.3, while by estimating release rate from dI_{post}/dt, N was 3.1 ± 0.5. The latter value is included in Table 2.

Although we applied many flashes to a single B2–B3 pair, there was no apparent order dependence, i.e. the responses fall on a single line relating release rate to $[Ca^{2+}]_i$, regardless of when a given $[Ca^{2+}]_i$ elevation occurred during an experiment and what stimuli preceded it. If there were a 'priming' or enhancement of release, due, for example, to processes such as post-tetanic potentiation, responses following prior flashes would have been larger than similar flashes early in the experiment. Conversely, synaptic depression would result in smaller responses to flashes of a given magnitude later in the experiment. Such effects would distort our measurement of stoichiometry, but they appear negligible on the time scale of the interval between flashes ($\geqslant$150 s).

Stoichiometry of Ca^{2+} action at peptidergic synapses (B2–SN)

We also performed NPE photolysis experiments on peptidergic synapses (B2–SN). Figure 4*A* shows three examples of flash-evoked presynaptic $[Ca^{2+}]_i$ rise and EPSCs. $[Ca^{2+}]_i$ was elevated rapidly after a flash, which was followed by recovery within 10–20 s to pre-flash levels as Ca^{2+} was pumped out of the presynaptic cell. In contrast to cholinergic IPSCs, peptidergic EPSCs outlasted the duration of the presynaptic $[Ca^{2+}]_i$ elevation, and postsynaptic SCP receptors did not desensitize over a similar time scale (Fig. 5*A*). Thus postsynaptic processes seem to be the main rate-limiting steps in determining response duration, and as with cholinergic synapses it is not possible to estimate accurately the time course of transmitter release. The slow decay of flash-evoked responses lasted 5–10 s longer than those to APs or brief SCP application (compare Fig. 4*Aa* to Figs 2*B* and 5*B*). This extension in duration is similar to the time of persistence of elevated $[Ca^{2+}]_i$, which occurs with spatial uniformity in photolysis experiments and is determined by the rate of Ca^{2+} removal by extrusion processes (Fig. 4*A*). Thus the duration of responses to photolysis is approximately the sum of the duration of the $[Ca^{2+}]_i$ rise and the postsynaptic responses to an AP or to brief peptide application. This suggests that some residual peptide release continues for the period of $[Ca^{2+}]_i$ elevation, persisting for over 20 s in photolysis experiments, but for a much shorter time in response to action potentials. Thus peptide secretion may continue for at least two orders of magnitude longer than cholinergic secretion in the presence of a persistent $[Ca^{2+}]_i$ elevation.

Unlike the case for cholinergic transmission (Fig. 3*A*), the maximum dI_{post}/dt occurs after the step in $[Ca^{2+}]_i$ begins to decline (Fig. 4*Ab*). This raises the question of which $[Ca^{2+}]_i$ triggers the peak dI_{post}/dt. If the 1–5 s delay in peak dI_{post}/dt is due to postsynaptic processes, then we should relate peak dI_{post}/dt to the previous peak level of $[Ca^{2+}]_i$. If, however, the delay in peak dI_{post}/dt reflects a delay in release, then perhaps it should be related to the simultaneously occurring $[Ca^{2+}]_i$.

To address this question, we measured the dI_{post}/dt of responses to 3 nM to 30 μM SCP_B puffed rapidly onto SN cells. The speed of solution change was shorter than 0.26 s (Fig. 5*Ab* and *Bb*, measured as a change in junction potential in an adjacent electrode to a dilute sea water perfusion), while dI_{post}/dt of peptidergic postsynaptic responses reached a peak after 1–5 s. Therefore, the delay in postsynaptic responses in *A* is due to postsynaptic factors, and so we relate peak dI_{post}/dt to the preceding peak $[Ca^{2+}]_i$ magnitude in Fig. 4.

In comparison to cholinergic synapses, a lower presynaptic $[Ca^{2+}]_i$ rise evoked by a dim flash elicited small but clear EPSCs. With a greater rise in $[Ca^{2+}]_i$ evoked by brighter flashes, EPSCs became larger and began to saturate (Fig. 4*B*). This saturation might arise from a limited readily releasable pool size, or saturation of some step in the postsynaptic response to peptides (see Fig. 5). However, there was no sign of saturation of peak dI_{post}/dt in Fig. 4*C*, since this maximum slope was measured well before saturation of the peak response. Therefore, stoichiometry of Ca^{2+} action was determined from the slope of dI_{post}/dt *vs.* $[Ca^{2+}]_i$ using eqn (3). The stoichiometry of 2.2 ± 0.6 is included in Table 2. As with cholinergic IPSCs, the Ca^{2+} dependence of peptidergic EPSCs appeared undistorted by effects of history-dependent enhancement or depression resulting from prior stimulation and $[Ca^{2+}]_i$ elevation; no such processes were evident at flash interval of $\geqslant$150 s.

Linear relationship between $[SCP_B]$ and maximum SN response

In classical fast synapses, such as those generating cholinergic EPSCs, transmitter release is quantized, and postsynaptic responses are linearly related to the number of quanta released, due to the largely non-overlapping postsynaptic action of transmitter quanta. This is true despite a frequently non-linear dependence of postsynaptic responses on transmitter concentration (Hartzell *et al.* 1976). However, peptidergic quanta are undetectable, and the linearity of summation of their postsynaptic effects is untested. If SN peptide receptors respond linearly to variation in [SCPs], then the issue of quantal overlap is moot and postsynaptic responses would be a valid detector of stoichiometry of presynaptic $[Ca^{2+}]_i$ in evoking transmitter release, at least at low, non-saturating peptide concentrations.

We measured the relationship between $[SCP_B]$ and peak dI_{post}/dt in single isolated SN cells. We used two puffing protocols. One involved a prolonged (60 s) application, allowing $[SCP_B]$ responses to achieve a steady inward current (Fig. 5*A*). No obvious desensitization was seen on this time scale, as shown previously (Whim *et al.* 1997). The other protocol involved a transient (1 s) application of peptide that better mimicked PSCs evoked by flash photolysis or an AP (Fig. 5*B*).

Figure 5*C* shows the dose–response curve for $[SCP_B]$ and the peak rate of inward current change. Using a 60 s application, the Hill coefficient was 0.85 ± 0.06, EC_{50} was 310 ± 70 nM, and maximal response level was

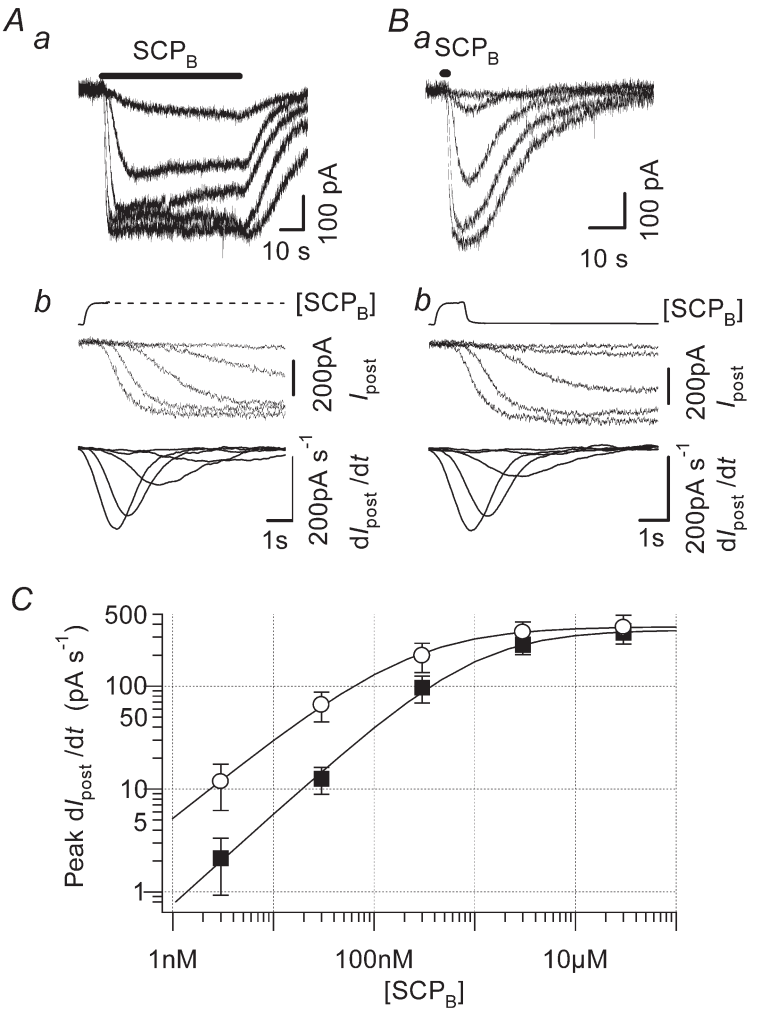

Figure 5. The SN is a linear, but delayed, detector of peptide

Aa, 60 s application of the peptide SCP_B at 3, 30 and 300 nM, and 3 and 30 μM (indicated by black bar) induced prolonged inward current in the SN. Desensitization was not observed. *Ba*, 1 s application of SCP_B (3 nM to 30 μM) mimics flash-evoked inward current in the same SN. *Ab* and *Bb* show the same responses (middle traces) and their derivatives (lower traces) on a faster time scale; upper traces track the time course of local concentration change (see Methods). *C*, dose–response curve for SCP_B concentration and the maximum rate of inward current change. The open circles represent 60 s application and filled squares represent 1 s applications of SCP_B. Lines are best-fit curves based on the Hill equation. Hill coefficients were 0.85 ± 0.06 (60 s application, $n = 4$) and 1.09 ± 0.09 (1 s application, $n = 6$).

400 ± 90 pA s^{-1} ($n = 4$). Using a 1 s application, the Hill coefficient was 1.09 ± 0.09, EC_{50} was 950 ± 420 nM, and maximal response level was 330 ± 70 pA s^{-1} ($n = 6$). Although there are no significant differences in the Hill coefficient, EC_{50}, or maximal response, the responses to low [SCP_B] appeared to be somewhat larger for 60 s peptide applications ($0.21 > P > 0.08$ for three points below 1 μM in Fig. 5*C*, Student's two-tailed *t* test). This is probably due to the slow rise time of small responses, reflecting slow on-kinetics of peptide binding or subsequent biochemical reactions underlying postsynaptic responses. Overall, the results indicate that the relationship between [SCP_B] and SN response is linear below a saturating level, and so should not distort measures of Ca^{2+} stoichiometry.

Figure 5 shows that at high [SCP_B] the postsynaptic responses saturate at peak dI_{post}/dt similar to response rates evoked by flash photolysis of presynaptic caged Ca^{2+} chelators (Fig. 4*C*). It might be wondered why the responses to flash photolysis do not saturate. One possibility is that the early phasic release of peptides in response to photolysis strongly excites receptors very briefly, and Fig. 5 shows that brief stimuli are less likely to saturate.

$[Ca^{2+}]_i$ 'thresholds' for cholinergic and peptidergic transmission

We searched for the minimum $[Ca^{2+}]_i$ required to elicit detectable responses to photolysis of NPE at cholinergic (B2–B3) and peptidergic (B2–SN) synapses. Figure 6 shows cholinergic and peptidergic transmission probabilities, which were plotted *versus* peak $[Ca^{2+}]_i$ elicited by flash photolysis. Transmission probability was calculated as follows: if photolysis seemed to elicit a postsynaptic response, it was marked as 1, and if not, it was marked as 0. Responses were scored using a blind procedure by three uninformed observers. Presynaptic $[Ca^{2+}]_i$ levels required to elicit postsynaptic responses (cholinergic: 6 pairs, 46 flashes; peptidergic: 9 pairs, 78 flashes) were binned, i.e. for a given range of $[Ca^{2+}]_i$, the transmission probability was computed as the average probability across observers of detecting a response. The threshold was set at a detected transmission probability of 0.5. Figure 6 and Table 2 show the results. Peptidergic synapses evoked detectable responses at lower $[Ca^{2+}]_i$ levels than cholinergic synapses.

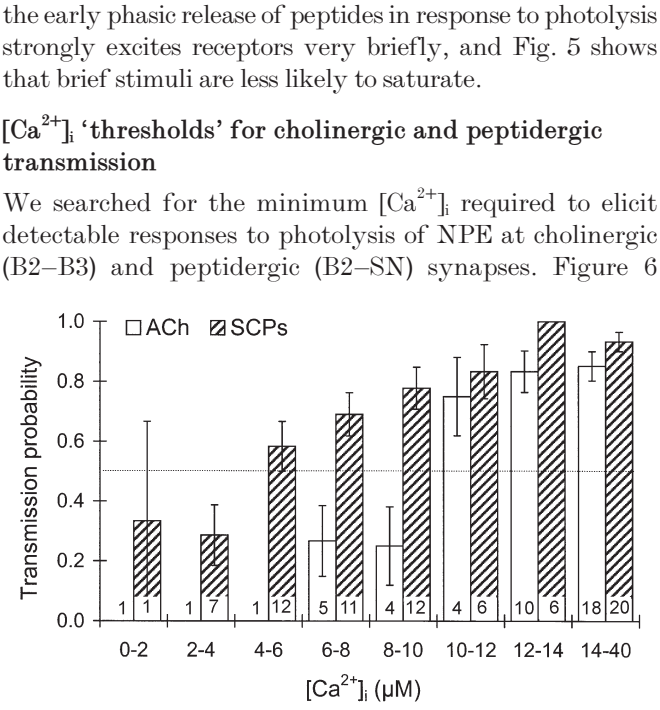

Figure 6. $[Ca^{2+}]_i$ level triggering minimally detectable cholinergic (B2–B3) and peptidergic (B2–SN) transmission

Probabilities of observing detectable cholinergic (open columns) and peptidergic (hatched columns) transmission were plotted *versus* peak $[Ca^{2+}]_i$ elicited by NPE photolysis. The $[Ca^{2+}]_i$ (at probability > 0.5) for triggering minimally detectable cholinergic transmission was about 10 μM and that for peptidergic transmission was less than 5 μM. Error bars represent S.E.M. of the ratings of 3 different individuals evaluating the data. The number within each bar represents the number of responses corresponding to $[Ca^{2+}]_i$ elevations within the range shown on the abscissa.

$[Ca^{2+}]_i$ at release sites elicited by an AP

We also estimated the $[Ca^{2+}]_i$ rise at release sites elicited by a single 5 ms suprathreshold depolarisation ($[Ca^{2+}]_{AP}$). APs induce a local $[Ca^{2+}]_i$ rise near Ca^{2+} channels, while flash photolysis induces a spatially uniform $[Ca^{2+}]_i$ rise. $[Ca^{2+}]_{AP}$ was calculated from the relationship between $[Ca^{2+}]_i$ and maximum release rate (eqn (3)) by normalizing responses in each preparation to those corresponding to a 10 μM rise in $[Ca^{2+}]_i$, according to:

$$N(\log[Ca^{2+}]_{AP} - \log 10\ \mu M) = \log r_{AP} - \log r_{10\mu M}, \qquad (4)$$

where r_{AP} is the peak release rate, measured as dI_{post}/dt, evoked by an AP, $r_{10\mu M}$ is the peak dI_{post}/dt at $[Ca^{2+}]_i = 10\ \mu M$, and N is the measured stoichiometry, both derived from NPE photolysis experiments. The results are shown in Table 2. The calculated $[Ca^{2+}]_{AP}$ of peptidergic synapses (8.8 μM) is less than that of cholinergic synapses (23 μM).

Table 2 shows that APs evoke peptidergic release at a maximum rate similar to that caused by a step rise in $[Ca^{2+}]_i$ to 10 μM, while APs evoke cholinergic release at a substantially higher maximum rate than that caused by a 10 μM step in $[Ca^{2+}]_i$. Application of eqn (4) suggests that the peak rise in $[Ca^{2+}]_i$ during APs is lower at the Ca^{2+} targets for peptidergic release sites than at the Ca^{2+} targets for cholinergic release. This would occur, for example, if cholinergic vesicles were localized in closer proximity to one or more Ca^{2+} channels than peptidergic vesicles. An alternative interpretation of the results is possible. If the on-rate of Ca^{2+} binding to the secretory trigger is slow enough, the transient $[Ca^{2+}]_i$ elevations in APs might evoke a lower maximal rate of release than a step of equal amplitude. Then eqn (4) provides an underestimate of the peak rise in $[Ca^{2+}]_i$ during an AP at the secretory trigger. It is even possible that peptidergic and cholinergic Ca^{2+} targets see equal $[Ca^{2+}]_i$ elevations during an AP, but that the binding of Ca^{2+} to peptidergic targets is much slower, resulting in less peptidergic secretion (compared to a step rise in $[Ca^{2+}]_i$) than cholinergic secretion. This possibility seems unlikely

because of the long durations of APs (5–10 ms), but it cannot be excluded.

Our estimates of $[Ca^{2+}]_i$ evoking release by an AP also depend on the validity of our calibration of BTC in the presence of NPE (Fig. 1). As explained in Methods, we believe the cuvette calibrations are more accurate than the *in situ* measurements. Using the *in situ* data without correction would result in estimates of $[Ca^{2+}]_i$ that are approximately twice as high as the estimates in Table 2. We think our cuvette calibrations are more relevant, but this is another source of uncertainty that could lead to underestimation of the levels of $[Ca^{2+}]_i$ reached in our experiments. However, such considerations do not affect estimates of the relative values of $[Ca^{2+}]_i$ evoking peptidergic and cholinergic release, and it is the difference in those values that we wish to emphasize.

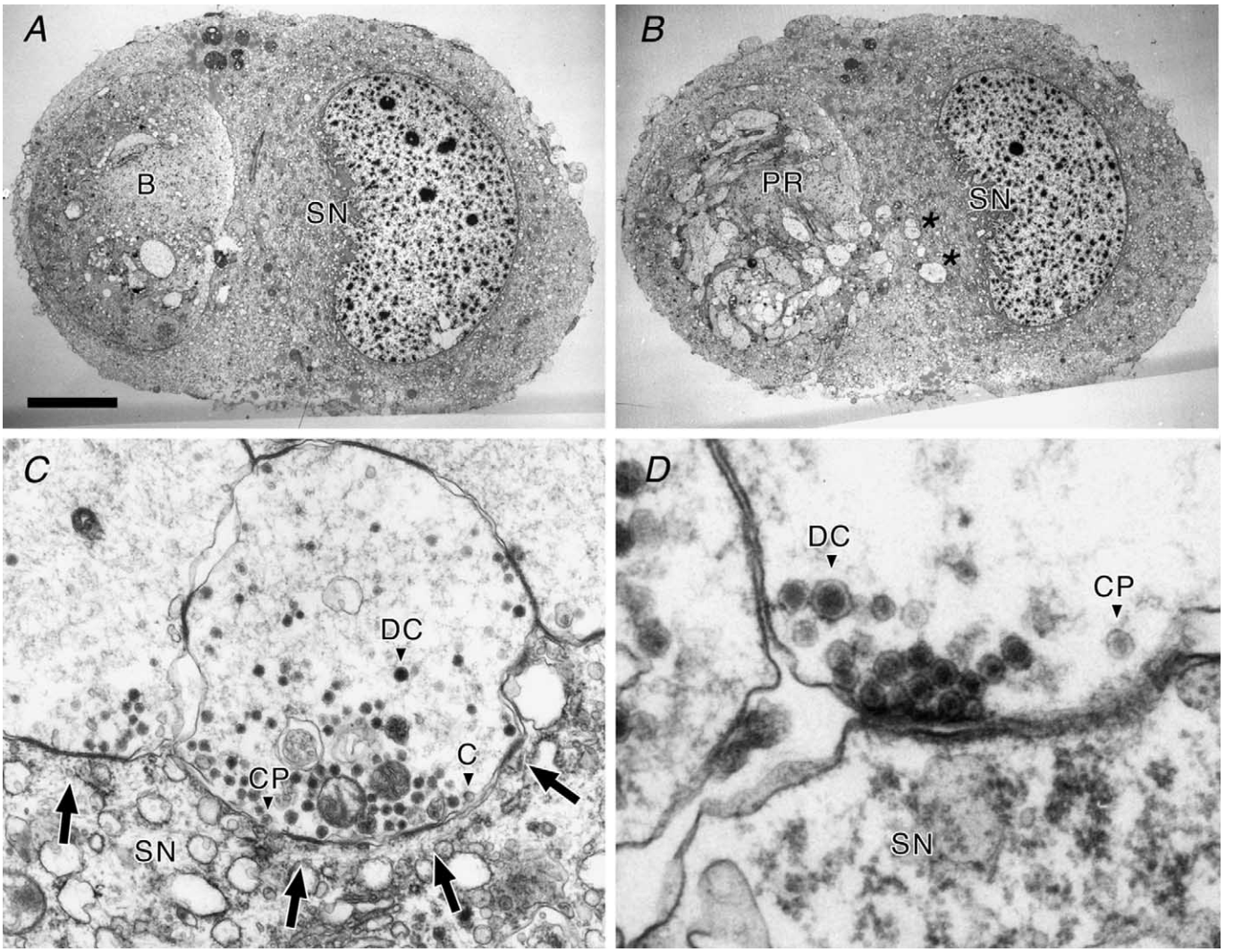

Figure 7. Electron microscopy of B2–SN neuron cell pair contacts

A, electron micrograph at the level of the SN and B2 cell somas. The left side ellipse is the B2 cell body (B); the right side ellipse is the nucleus of the SN (SN). Note the complete envelopment of the B2 cell body within the sensory neuron cell body. *B*, electron micrograph at the level of contact between the SN soma (SN) and processes of the B2 axon stump. Neuronal processes were found largely in a neuropil-like bundle of neuronal processes (PR) at the edge of the SN cell, but a few individual B2 processes were also observed within the soma (asterisks). *C*, electron micrograph of the contact between several bouton-like processes and a sensory neuron (SN) cell. The membrane contact region shows localized regions of increased staining density and thickening (arrows), resembling the membrane specializations normally characteristic of active zones. Examples of the three vesicle types observed in this study are indicated by labelled arrowheads: dense-core (DC), compound (CP) and clear (C) vesicle. *D*, electron micrograph of a single active zone-like specialization in a 'bouton'/sensory neuron soma contact. In this case, the vesicles are very tightly clustered and localized quite near to the more densely staining region of the membrane. Both dense core (DC) and compound vesicles (CP) can be seen, and many DC vesicles are docked within active zones. Scale bar: *A* and *B*, 10 μm; *C*, 500 nm; *D*, 135 nm.

Our calculations require that ACh released by APs and NPE photolysis activate the same class of ACh receptors. ACh responses in *Aplysia* consist of two components: an early and rapidly desensitizing component (to prolonged ACh application) that is blocked by α-conotoxin ImI, and a later persistent component resistant to α-conotoxin ImI (Kehoe & McIntosh, 1998). Maximum rates of dI_{post}/dt occurred within less than 50 ms of the stimulus, when the fast component is typically ⩾ 5 times the magnitude of the slow component. We confirmed that both AP- and photolysis-evoked ACh responses are dominated by action at the fast, desensitizing ACh receptors by showing that both responses are largely blocked by 5 μM α-conotoxin ImI, especially at times when maximum dI_{post}/dt was measured (data not shown).

Ultrastructure of peptidergic synapses

Several B2–SN cell pairs were examined by electron microscopy to determine the nature of the synaptic contacts that develop in culture (Fig. 7). We were particularly interested in locating the structural basis (docked vesicles?) underlying peptidergic responses to single APs. Serial sections were cut along an axis perpendicular to the two cell somas in order to examine the region of contact. In sections of B2–SN pairs containing the two cell somata (Fig. 7*A*), thin cytoplasmic processes from the SN cell resembling lamellipodia were frequently seen to enwrap the soma of B2. In contrast, in sections containing the sensory neuron soma and the regenerated process of the B2 cell, these cytoplasmic extensions from SN contacted B2 processes but did not completely enwrap them. In addition, we observed arrays of presynaptic B2 processes in contact with and sometimes embedded in the SN soma (Fig. 7*B*, asterisks).

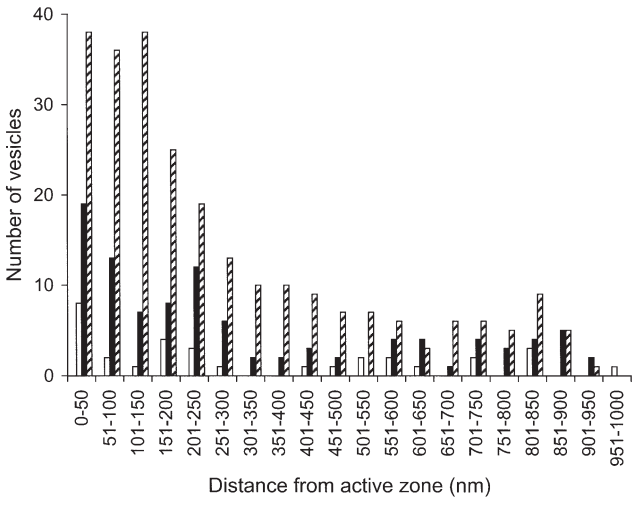

Figure 8. Spatial distribution of clear (open bars), dense core (black bars) and compound (hatched bars) synaptic vesicles in or near 17 active zones

Within the first 50 nm of the plasma membrane bounding an active zone, the region in which vesicles are considered 'docked', clear vesicles account for 12%, dense core vesicles for 30%, and compound vesicles for 58% of the total number of vesicles.

In regions of contact between B2 and SN, many of the B2 processes formed expanded bouton-like contacts with the SN soma (Fig. 7*C*) that resembled synapses described previously in *Aplysia* neuron cultures (Klein, 1994). In addition to mitochondria and extensive arrays of microtubules, many of the neuronal processes and all of the bouton-like structures contained three types of vesicles: DCVs 73.3 ± 1.0 nm in diameter (mean ± S.E.M., $n = 101$), electron-lucent vesicles 53.3 ± 1.8 nm in diameter (mean ± S.E.M., $n = 27$), and compound vesicles 58.0 ± 0.5 nm in diameter (mean ± S.E.M., $n = 232$) similar in morphology to those described previously by Reed *et al.* (1988). Roughly 92% of the vesicles were of the DCV or compound type – of these about 30% were DCVs and 70% were compound. The size differences between the vesicle types were statistically significant ($P < 0.01$, unpaired t test).

All three vesicle types were also found in the somata of the B2 cells, but at lower density than in the processes. In contrast, the SN cell somata contained almost exclusively electron-lucent vesicles. These observations suggest that the bouton-like structures originate from cell B2, rather than from SN cells.

In 23 random micrographs taken of the B2–SN contact region in four different cell pairs, 17 of the 23, or 74%, showed bouton-like processes in contact with the SN soma with one or more morphologically 'docked' vesicle (vesicle within one vesicle diameter of the neuronal membrane). In many of these instances, there were large numbers of vesicles close to the membrane of the neuronal process along nearly the entire length of the neuronal process–soma contact (Fig. 7*C*). The zone of contact between the SN membrane and the bouton-like process was also characterized by short lengths of more densely stained membrane (Fig. 7*C*, arrows) resembling the membrane thickenings of classical fast synaptic contacts. At some of these vesicle-rich, darkly staining membrane contacts, the vesicles were so tightly clustered at a single site and near the membrane that they could be called conventional 'active zones'. Many of these 'active zones' contained clear and compound vesicles, as previously reported by Klein (1994), but some were composed almost exclusively of DCVs (Fig. 7*D*).

To quantify the distribution of vesicles in and near active zones, we examined the spatial distribution of synaptic vesicles from the plasma membrane of 17 active zones. Counts of synaptic vesicles around active zones were used to construct a vesicle localization histogram (Fig. 8). Substantial fractions of each vesicle type (25% of clear, 18% of DCV, and 15% of compound vesicles) had their centres within 50 nm (less than one DCV diameter) of the plasma membrane within the active zone, the region in which they were considered morphologically 'docked' (Reist

et al. 1998). The clustering of vesicles near the membrane was statistically significant for all three vesicle types ($P < 0.0013$, χ^2 test). Furthermore, 21 % of the 'docked' DCVs and 39 % of the 'docked' compound vesicles appeared to be in direct contact with the active zone membrane.

DISCUSSION

The ability of *Aplysia* buccal ganglion cell B2 to form cholinergic or peptidergic synapses with different target neurons allowed us to compare the Ca^{2+} dependence of transmitter release at fast and slow synapses formed by the same presynaptic neuron. The chief differences in Ca^{2+} sensitivity between cholinergic and peptidergic secretion from cell B2 are summarized in Table 2. Peptidergic transmission was characterized by an apparently slightly lower Ca^{2+} stoichiometry, and smaller $[Ca^{2+}]_i$ levels for activating both minimal responses and responses similar to those of an action potential.

Peptidergic transmission was also slower than cholinergic transmission, due mainly to properties of the postsynaptic receptors and additional enzymatic reactions preceding modulation of ion channels by peptidergic receptors (Baxter & Byrne, 1989). Unlike cholinergic release, some peptidergic transmission appeared to persist during prolonged $[Ca^{2+}]_i$ elevation. This may reflect differences in the sizes of reserve pools of peptidergic and cholinergic vesicles or in the rates that immediately releasable pools can be replenished. Desensitisation of cholinergic receptors is not likely to be involved, because desensitisation is neither as fast as nor as complete as the decay of cholinergic responses (Kehoe & McIntosh, 1998). A more remote possibility is that some presynaptic process unique to cholinergic terminals intervenes to shut down transmitter release shortly after $[Ca^{2+}]_i$ concentration rises.

Comparison to other preparations

Cholinergic transmission from cell B2 to B6 can be compared to other fast (glutamatergic) synapses involving small synaptic vesicles, studied in goldfish bipolar neurons (Heidelberger *et al.* 1994), crayfish neuromuscular junctions (Landò & Zucker, 1994), and rat medial trapezoid body nucleus calyx of Held synapses (Bollmann *et al.* 2000; Schneggenburger & Neher, 2000), and to ACh release from PC12 cells (Kasai *et al.* 1996; Ninomiya *et al.* 1997). In all cases, Ca^{2+} stoichiometries of 3–4 have been reported, similar to our measurement. Our estimate of 23 μM $[Ca^{2+}]_i$ triggering release in an AP, which we have argued is likely to be an underestimate, may be compared to values of 9–25 μM at the calyx of Held and 20 μM at crayfish neuromuscular junctions. The latter value, which was originally estimated at 75 μM based on calculations from models of DM-nitrophen photolysis in cytoplasm, has been revised downward due to revision of the Mg^{2+}-binding constants of DM-nitrophen (Ayer & Zucker, 1999) and the native buffer power (Tank *et al.* 1995) used in deriving this estimate. At goldfish bipolar synapses, fast rates of release appeared to require $[Ca^{2+}]_i$ levels approaching the half-maximal level of 200 μM, while half-maximal ACh release from PC12 cells occurred at 25 μM. Our estimate of 10 μM $[Ca^{2+}]_i$ needed to evoke a minimum phasic release of ACh may be compared to a level of 20 μM at bipolar synapses and over 10 μM for ACh release from PC12 cells. It should be noted, however, that submicromolar $[Ca^{2+}]_i$ levels were sufficient to evoke tonic increases in transmission at goldfish bipolar (Lagnado *et al.* 1996) and salamander photoreceptor (Rieke & Schwartz, 1996) synapses, similar to levels needed to substantially increase the frequency of miniature synaptic potentials at crayfish neuromuscular junctions (Delaney & Tank, 1994; Ravin *et al.* 1997).

We know of no comparable study of the $[Ca^{2+}]_i$ dependence of transmitter release from a peptidergic neuron. However, peptidergic transmission from B2 onto SN, involving DCVs, may be compared to non-synaptic release of catecholamines or peptides from endocrine and neurosecretory cells, including noradrenaline release from bovine chromaffin cells (Heinemann *et al.* 1994) and PC12 cells (Kasai *et al.* 1996; Ninomiya *et al.* 1997), vassopressin release from posterior pituitary cells (Cazalis *et al.* 1987; Lindau *et al.* 1992), peptide secretion from pituitary melanotrophs (Thomas *et al.* 1993) and corticotrophs (Tse *et al.* 1997), and insulin secretion from pancreatic β-cells (Proks *et al.* 1996). Our estimated stoichiometry of 2.2 falls within the reported range of Ca^{2+} stoichiometries – as low as 1.5 in posterior pituitary cells to 2.5–5 for the other cell types. More indirect experiments inferred a linear Ca^{2+} dependence of peptide secretion from rat motor neurons (Sakaguchi *et al.* 1991) and bullfrog sympathetic neurons (Peng & Zucker, 1993). Our estimate of 9 μM $[Ca^{2+}]_i$ triggering release to an AP might be compared to half-maximal $[Ca^{2+}]_i$ levels as low as 2 μM in the posterior pituitary, 8 μM in PC12 cells, 15 μM in corticotrophs, and 27 μM in melanotrophs, while $[Ca^{2+}]_i$ appears to reach 10 μM during brief depolarisations in chromaffin cells (Chow *et al.* 1994). Finally, our estimate of 5 μM as the $[Ca^{2+}]_i$ threshold needed to evoke a minimal response falls within the range of about 0.5 μM in posterior pituitary and chromaffin cells to 5 μM in PC12 cells. It must be acknowledged that neither our estimates of $[Ca^{2+}]_i$ involved in triggering transmitter release nor most of those in the literature are terribly precise. In general, our finding of lower Ca^{2+} stoichiometry, lower level achieved at release sites during an AP or levels needed for half-maximal release, and lower $[Ca^{2+}]_i$ needed to activate minimal release, in peptidergic compared to cholinergic synapses, resembles the average differences between fast and slow secretion gleaned from the literature (see also Verhage *et al.* 1991). However, only in the PC12 tumour cell line has it been possible to quantitatively compare fast (cholinergic) and slow (noradrenergic) secretion (Kasai *et al.* 1996).

The differences between cholinergic and peptidergic secretion are suited to the different needs of fast and slow

synapses. Our ultrastructural results suggest that both types of transmission may occur at active zones, and involve vesicles docked at the membrane, which is consistent with our finding that the Ca^{2+} dependence of cholinergic and peptidergic transmission were not as different as we had expected. In this regard it is interesting that both cholinergic and DCV secretion involve the function of similar SNARE proteins, including syntaxin, synaptobrevin, SNAP-25, and CAPS (Martin & Kowalchyk, 1997; Whim *et al.* 1997). However, our proposal of a higher level of $[Ca^{2+}]_i$ triggering ACh secretion than SCP secretion, as well as our estimate of a higher 'threshold' $[Ca^{2+}]_i$ level for triggering minimal phasic release, suggests that cholinergic vesicles are more closely tied to Ca^{2+} channels than DCVs containing SCPs, or are exposed to greater overlap of Ca^{2+} channel microdomains due to a higher local density of Ca^{2+} channels. This allows for a more rapid rise in $[Ca^{2+}]_i$ at cholinergic secretory trigger sites, necessary for fast secretion. Ca^{2+} stoichiometry at cholinergic synapses appeared to be somewhat higher than that at peptidergic synapses (although the difference did not reach statistical significance, $P = 0.29$, two-tailed t test). A higher stoichiometry suggests the requirement for cooperative binding of more Ca^{2+} ions in triggering small cholinergic vesicle fusion than in triggering peptidergic vesicle fusion, which aids in producing large rates of release that terminate rapidly as local $[Ca^{2+}]_i$ levels drop following an AP.

Docked peptidergic DCVs

Our observation of apparently docked DCVs in active zones contrasts with the common assertion that neuronal DCVs are rarely if ever docked at the membrane, and are excluded from active zones (De Camilli & Jahn, 1990; Verhage *et al.* 1991; Golding, 1994; Karhunen *et al.* 2000; but see Sharman *et al.* 2000). The fact that single APs, short trains, or brief depolarizations often fail to release detectable amounts of peptide (Whim & Lloyd, 1989, 1994; Seward *et al.* 1995; Vilim *et al.* 1996; Leenders *et al.* 1999) has often been attributed to an absence of docked vesicles ready for release. B2 appears to be unusual in this regard, in that it contains DCVs docked in active zones, and single APs evoke clear postsynaptic responses (Whim *et al.* 1997). In B2's peptidergic synapses, a substantial number of vesicles are docked in active zones, and in reasonably close proximity to Ca^{2+} channels. This conclusion is indicated by our estimate of the approximately 10 μM $[Ca^{2+}]_i$ (or more if the binding of Ca^{2+} to the secretory trigger is slow) reached at the Ca^{2+} target for peptidergic release, likely to be on vesicles or their docking complex. It is also supported by the ability of peptidergic synapses to transmit to single APs even when presynaptic cells contain 5 mM NPE, a powerful Ca^{2+} buffer. When loaded with 3.75 mM Ca^{2+}, this leaves 1.25 mM free NPE to buffer incoming Ca^{2+}. Such an EGTA concentration has a profound effect on secretion from chromaffin cells (Seward & Nowycky, 1996; Klingauf & Neher, 1997), which have no active zones, but has less or no effect on release of fast transmitters in a variety of neurons (Delaney *et al.* 1991; Swandulla *et al.* 1991; Borst & Sakmann, 1996). Thus at least some peptidergic vesicles are docked near Ca^{2+} channels and primed for immediate release, although they may be less precisely co-localized than are cholinergic vesicles with those channels.

Adler, E. M., Augustine, G. J., Duffy, S. N. & Charlton, M. P. (1991). Alien intracellular calcium chelators attenuate neurotransmitter release at the squid giant synapse. *Journal of Neuroscience* **11**, 1496–1507.

Augustine, G. J., Charlton, M. P. & Smith, S. J. (1985). Calcium entry and transmitter release at voltage-clamped nerve terminals of squid. *Journal of Physiology* **367**, 163–181.

Ayer, R. K. Jr & Zucker, R. S. (1999). Magnesium binding to DM-nitrophen and its effect on the photorelease of calcium. *Biophysical Journal* **77**, 3384–3393.

Baxter, D. A. & Byrne, J. H. (1989). Serotonergic modulation of two potassium currents in the pleural sensory neurons of *Aplysia*. *Journal of Neurophysiology* **62**, 665–679.

Bollmann, J. H., Sakmann, B. & Borst, J. G. (2000). Calcium sensitivity of glutamate release in a calyx-type terminal. *Science* **289**, 953–957.

Borst, J. G. & Sakmann, B. (1996). Calcium influx and transmitter release in a fast CNS synapse. *Nature* **383**, 431–434.

Carrow, G. M. & Levitan, I. B. (1989). Selective formation and modulation of electrical synapses between cultured *Aplysia* neurons. *Journal of Neuroscience* **9**, 3657–3664.

Cazalis, M., Dayanithi, G. & Nordmann, J. J. (1987). Requirements for hormone release from permeabilized nerve endings isolated from the rat neurohypophysis. *Journal of Physiology* **390**, 71–91.

Chow, R. H., Klingauf, J. & Neher, E. (1994). Time course of Ca^{2+} concentration triggering exocytosis in neuroendocrine cells. *Proceedings of the National Academy of Sciences of the USA* **91**, 12765–12769.

Church, P. J., Whim, M. D. & Lloyd, P. E. (1993). Modulation of neuromuscular transmission by conventional and peptide transmitters released from excitatory and inhibitory motor neurons in *Aplysia*. *Journal of Neuroscience* **13**, 2790–2800.

Cropper, E. C., Price, D., Tenenbaum, R., Kupfermann, I. & Weiss, K. R. (1990). Release of peptide cotransmitters from a cholinergic motor neuron under physiological conditions. *Proceedings of the National Academy of Sciences of the USA* **87**, 933–937.

De Camilli, P. & Jahn, R. (1990). Pathways to regulated exocytosis in neurons. *Annual Review of Physiology* **52**, 625–645.

Delaney, K., Tank, D. W. & Zucker, R. S. (1991). Presynaptic calcium and serotonin-mediated enhancement of transmitter release at crayfish neuromuscular junction. *Journal of Neuroscience* **11**, 2631–2643.

Delaney, K. R. & Tank, D. W. (1994). A quantitative measurement of the dependence of short-term synaptic enhancement on presynaptic residual calcium. *Journal of Neuroscience* **14**, 5885–5902.

Delprincipe, F., Egger, M., Ellis-Davies, G. C. & Niggli, E. (1999). Two-photon and UV-laser flash photolysis of the Ca^{2+} cage, dimethoxynitrophenyl-EGTA-4. *Cell Calcium* **25**, 85–91.

Dodge, F. A. Jr & Rahamimoff, R. (1967). Co-operative action of calcium ions in transmitter release at the neuromuscular junction. *Journal of Physiology* **193**, 419–432.

Dudel, J. (1981). The effect of reduced calcium on quantal unit current and release at the crayfish neuromuscular junction. *Pflügers Archiv* **391**, 35–40.

Dutton, A. & Dyball, R. E. (1979). Phasic firing enhances vasopressin release from the rat neurohypophysis. *Journal of Physiology* **290**, 433–440.

Ellis-Davies, G. C. & Kaplan, J. H. (1994). Nitrophenyl-EGTA, a photolabile chelator that selectively binds Ca^{2+} with high affinity and releases it rapidly upon photolysis. *Proceedings of the National Academy of Sciences of the USA* **91**, 187–191.

Fenwick, E. M., Marty, A. & Neher, E. (1982). A patch-clamp study of bovine chromaffin cells and of their sensitivity to acetylcholine. *Journal of Physiology* **331**, 577–597.

Gardner, D. & Kandel, E. R. (1977). Physiological and kinetic properties of cholinergic receptors activated by multiaction interneurons in buccal ganglia of *Aplysia*. *Journal of Neurophysiology* **40**, 333–348.

Golding, D. W. (1994). A pattern confirmed and refined – synaptic, nonsynaptic and parasynaptic exocytosis. *Bioessays* **16**, 503–508.

Grynkiewicz, G., Poenie, M. & Tsien, R. Y. (1985). A new generation of Ca^{2+} indicators with greatly improved fluorescence properties. *Journal of Biological Chemistry* **260**, 3440–3450.

Hartzell, H. C., Kuffler, S. W. & Yoshikami, D. (1976). The number of acetylcholine molecules in a quantum and the interaction between quanta at the subsynaptic membrane of the skeletal neuromuscular synapse. *Cold Spring Harbor Symposia on Quantitative Biology* **40**, 175–186.

Haydon, P. G. (1988). The formation of chemical synapses between cell-cultured neuronal somata. *Journal of Neuroscience* **8**, 1032–1038.

Heidelberger, R., Heinemann, C., Neher, E. & Matthews, G. (1994). Calcium dependence of the rate of exocytosis in a synaptic terminal. *Nature* **371**, 513–515.

Heinemann, C., Chow, R. H., Neher, E. & Zucker, R. S. (1994). Kinetics of the secretory response in bovine chromaffin cells following flash photolysis of caged Ca^{2+}. *Biophysical Journal* **67**, 2546–2557.

Hess, S. D., Doroshenko, P. A. & Augustine, G. J. (1993). A functional role for GTP-binding proteins in synaptic vesicle cycling. *Science* **259**, 1169–1172.

Hsu, S. F., Augustine, G. J. & Jackson, M. B. (1996). Adaptation of Ca^{2+}-triggered exocytosis in presynaptic terminals. *Neuron* **17**, 501–512.

Iatridou, H., Foukaraki, E., Kuhn, M. A., Marcus, E. M., Haugland, R. P. & Katerinopoulos, H. E. (1994). The development of a new family of intracellular calcium probes. *Cell Calcium* **15**, 190–198.

Jan, L. Y. & Jan, Y. N. (1982). Peptidergic transmission in sympathetic ganglia of the frog. *Journal of Physiology* **327**, 219–246.

Karhunen, T., Vilim, F. S., Alexeeva, V., Weiss, K. R. & Church, P. J. (2000). Targeting of peptidergic vesicles in cotransmitting terminals. *Journal of Neuroscience* **21**, 1–5.

Kasai, H., Takagi, H., Ninomiya, Y., Kishimoto, T., Ito, K., Yoshida, A., Yoshioka, T. & Miyashita, Y. (1996). Two components of exocytosis and endocytosis in phaeochromocytoma cells studied using caged Ca^{2+} compounds. *Journal of Physiology* **494**, 53–65.

Katz, B. & Miledi, R. (1970). Further study of the role of calcium in synaptic transmission. *Journal of Physiology* **207**, 789–801.

Kehoe, J. & McIntosh, J. M. (1998). Two distinct nicotinic receptors, one pharmacologically similar to the vertebrate α7-containing receptor, mediate Cl currents in *Aplysia* neurons. *Journal of Neuroscience* **18**, 8198–8213.

Klein, M. (1994). Synaptic augmentation by 5-HT at rested *Aplysia* sensorimotor synapses: independence of action potential prolongation. *Neuron* **13**, 159–166.

Klingauf, J. & Neher, E. (1997). Modeling buffered Ca^{2+} diffusion near the membrane: implications for secretion in neuroendocrine cells. *Biophysical Journal* **72**, 674–690.

Kreiner, T., Sossin, W. & Scheller, R. H. (1986). Localization of *Aplysia* neurosecretory peptides to multiple populations of dense core vesicles. *Journal of Cell Biology* **102**, 769–782.

Krishtal, O. A. & Pidoplichko, V. I. (1980). A receptor for protons in the nerve cell membrane. *Neuroscience* **5**, 2325–2327.

Kupfermann, I. (1991). Functional studies of cotransmission. *Physiological Reviews* **71**, 683–732.

Lagnado, L., Gomis, A. & Job, C. (1996). Continuous vesicle cycling in the synaptic terminal of retinal bipolar cells. *Neuron* **17**, 957–967.

Landò, L. & Zucker, R. S. (1989). "Caged calcium" in *Aplysia* pacemaker neurons. Characterization of calcium-activated potassium and nonspecific cation currents. *Journal of General Physiology* **93**, 1017–1060.

Landò, L. & Zucker, R. S. (1994). Ca^{2+} cooperativity in neurosecretion measured using photolabile Ca^{2+} chelators. *Journal of Neurophysiology* **72**, 825–830.

Leenders, A. G., Scholten, G., Wiegant, V. M., Da Silva, F. H. & Ghijsen, W. E. (1999). Activity-dependent neurotransmitter release kinetics: correlation with changes in morphological distributions of small and large vesicles in central nerve terminals. *European Journal of Neuroscience* **11**, 4269–4277.

Lindau, M., Stuenkel, E. L. & Nordmann, J. J. (1992). Depolarization, intracellular calcium and exocytosis in single vertebrate nerve endings. *Biophysical Journal* **61**, 19–30.

Llinás, R., Sugimori, M. & Silver, R. B. (1992). Presynaptic calcium concentration microdomains and transmitter release. *Journal de Physiologie* **86**, 135–138.

Lloyd, P. E., Mahon, A. C., Kupfermann, I., Cohen, J. L., Scheller, R. H. & Weiss, K. R. (1985). Biochemical and immunocytological localization of molluscan small cardioactive peptides in the nervous system of *Aplysia californica*. *Journal of Neuroscience* **5**, 1851–1861.

Lloyd, P. E., Schacher, S., Kupfermann, I. & Weiss, K. R. (1986). Release of neuropeptides during intracellular stimulation of single identified *Aplysia* neurons in culture. *Proceedings of the National Academy of Sciences of the USA* **83**, 9794–9798.

Martin, T. F. & Kowalchyk, J. A. (1997). Docked secretory vesicles undergo Ca^{2+}-activated exocytosis in a cell-free system. *Journal of Biological Chemistry* **272**, 14447–14453.

Neher, E. & Zucker, R. S. (1993). Multiple calcium-dependent processes related to secretion in bovine chromaffin cells. *Neuron* **10**, 21–30.

Ninomiya, Y., Kishimoto, T., Yamazawa, T., Ikeda, H., Miyashita, Y. & Kasai, H. (1997). Kinetic diversity in the fusion of exocytotic vesicles. *EMBO Journal* **16**, 929–934.

Ocorr, K. A. & Byrne, J. H. (1985). Membrane responses and changes in cAMP levels in *Aplysia* sensory neurons produced by serotonin, tryptamine, FMRFamide and small cardioactive peptide$_B$ (SCP$_B$). *Neuroscience Letters* **55**, 113–118.

Peng, Y. Y. & Horn, J. P. (1991). Continuous repetitive stimuli are more effective than bursts for evoking LHRH release in bullfrog sympathetic ganglia. *Journal of Neuroscience* **11**, 85–95.

Peng, Y. Y. & Zucker, R. S. (1993). Release of LHRH is linearly related to the time integral of presynaptic Ca^{2+} elevation above a threshold level in bullfrog sympathetic ganglia. *Neuron* **10**, 465–473.

Proks, P., Eliasson, L., Ammala, C., Rorsman, P. & Ashcroft, F. M. (1996). Ca^{2+}- and GTP-dependent exocytosis in mouse pancreatic β-cells involves both common and distinct steps. *Journal of Physiology* **496**, 255–264.

Ravin, R., Spira, M. E., Parnas, H. & Parnas, I. (1997). Simultaneous measurement of intracellular Ca^{2+} and asynchronous transmitter release from the same crayfish bouton. *Journal of Physiology* **501**, 251–262.

Reed, W., Weiss, K. R., Lloyd, P. E., Kupfermann, I., Chen, M. & Bailey, C. H. (1988). Association of neuroactive peptides with the protein secretory pathway in identified neurons of *Aplysia californica*: immunolocalization of SCP$_A$ and SCP$_B$ to the contents of dense-core vesicles and the trans face of the Golgi apparatus. *Journal of Comparative Neurology* **272**, 358–369.

Reist, N. E., Buchanan, J., Li, J., Diantonio, A., Buxton, E. M. & Schwarz, T. L. (1998). Morphologically docked synaptic vesicles are reduced in *synaptotagmin* mutants of *Drosophila*. *Journal of Neuroscience* **18**, 7662–7673.

Rieke, F. & Schwartz, E. A. (1996). Asynchronous transmitter release: control of exocytosis and endocytosis at the salamander rod synapse. *Journal of Physiology* **493**, 1–8.

Roberts, W. M., Jacobs, R. A. & Hudspeth, A. J. (1990). Colocalization of ion channels involved in frequency selectivity and synaptic transmission at presynaptic active zones of hair cells. *Journal of Neuroscience* **10**, 3664–3684.

Sakaguchi, M., Inaishi, Y., Kashihara, Y. & Kuno, M. (1991). Release of calcitonin gene-related peptide from nerve terminals in rat skeletal muscle. *Journal of Physiology* **434**, 257–270.

Sato, T. (1968). A modified method for lead staining of thin sections. *Journal of Electron Microscopy* **17**, 158–159.

Schacher, S. & Proshansky, E. (1983). Neurite regeneration by *Aplysia* neurons in dissociated cell culture: modulation by *Aplysia* hemolymph and the presence of the initial axonal segment. *Journal of Neuroscience* **3**, 2403–2413.

Schneggenburger, R. & Neher, E. (2000). Intracellular calcium dependence of transmitter release rates at a fast central synapse. *Nature* **406**, 889–893.

Seward, E. P., Chernevskaya, N. I. & Nowycky, M. C. (1995). Exocytosis in peptidergic nerve terminals exhibits two calcium-sensitive phases during pulsatile calcium entry. *Journal of Neuroscience* **15**, 3390–3399.

Seward, E. P. & Nowycky, M. C. (1996). Kinetics of stimulus-coupled secretion in dialyzed bovine chromaffin cells in response to trains of depolarizing pulses. *Journal of Neuroscience* **16**, 553–562.

Sharman, A., Hirji, R., Birmingham, J. T. & Govind, C. K. (2000). Crab stomach pyloric muscles display not only excitatory but inhibitory and neuromodulatory nerve terminals. *Journal of Comparative Neurology* **425**, 70–81.

Swandulla, D., Hans, M., Zipser, K. & Augustine, G. J. (1991). Role of residual calcium in synaptic depression and posttetanic potentiation: fast and slow calcium signaling in nerve terminals. *Neuron* **7**, 915–926.

Tank, D. W., Regehr, W. G. & Delaney, K. R. (1995). A quantitative analysis of presynaptic calcium dynamics that contribute to short-term enhancement. *Journal of Neuroscience* **15**, 7940–7952.

Thomas, P., Wong, J. G., Lee, A. K. & Almers, W. (1993). A low affinity Ca^{2+} receptor controls the final steps in peptide secretion from pituitary melanotrophs. *Neuron* **11**, 93–104.

Tse, F. W., Tse, A., Hille, B., Horstmann, H. & Almers, W. (1997). Local Ca^{2+} release from internal stores controls exocytosis in pituitary gonadotrophs. *Neuron* **18**, 121–132.

Van der Kloot, W. (1988). Estimating the timing of quantal releases during end-plate currents at the frog neuromuscular junction. *Journal of Physiology* **402**, 595–603.

Verhage, M., McMahon, H. T., Ghijsen, W. E., Boomsma, F., Scholten, G., Wiegant, V. M. & Nicholls, D. G. (1991). Differential release of amino acids, neuropeptides, and catecholamines from isolated nerve terminals. *Neuron* **6**, 517–524.

Vilim, F. S., Cropper, E. C., Price, D. A., Kupfermann, I. & Weiss, K. R. (1996). Release of peptide cotransmitters in *Aplysia*: regulation and functional implications. *Journal of Neuroscience* **16**, 8105–8114.

Whim, M. D. & Lloyd, P. E. (1989). Frequency-dependent release of peptide cotransmitters from identified cholinergic motor neurons in *Aplysia*. *Proceedings of the National Academy of Sciences of the USA* **86**, 9034–903.

Whim, M. D. & Lloyd, P. E. (1994). Differential regulation of the release of the same peptide transmitters from individual identified motor neurons in culture. *Journal of Neuroscience* **14**, 4244–4251.

Whim, M. D., Niemann, H. & Kaczmarek, L. K. (1997). The secretion of classical and peptide cotransmitters from a single presynaptic neuron involves a synaptobrevin-like molecule. *Journal of Neuroscience* **17**, 2338–2347.

Zhao, M., Hollingworth, S. & Baylor, S. M. (1996). Properties of tri- and tetracarboxylate Ca^{2+} indicators in frog skeletal muscle fibers. *Biophysical Journal* **70**, 896–916.

Zucker, R. (1994). Photorelease techniques for raising or lowering intracellular Ca^{2+}. *Methods in Cell Biology* **40**, 31–63.

Zucker, R. S. (1992). Effects of photolabile calcium chelators on fluorescent calcium indicators. *Cell Calcium* **13**, 29–40.

Zucker, R. S. (1993). The calcium concentration clamp: spikes and reversible pulses using the photolabile chelator DM-nitrophen. *Cell Calcium* **14**, 87–100.

Acknowledgements

We thank Dr Paul J. Church (Mt Sinai School of Medicine, New York) for valuable suggestions on culturing *Aplysia* neurons, Dr. William Gilly (Hopkins Marine Station, Pacific Grove, CA, USA) for advice on patching *Aplysia* neurons, and Dr Graham C. R. Ellis-Davies (Medical College of Pennsylvania Hahnemann University, Philadelphia, PA, USA) for a gift of NPE and DMNPE-4. This work was supported by U.S. National Institutes of Health Grant NS15114.

Corresponding author

R. S. Zucker: Molecular and Cell Biology Department, 111 Life Sciences Addition, University of California, Berkeley, CA 94720-3200, USA.

Email: zucker@socrates.berkeley.edu